

EAGLE: Elevating Geometric Reasoning through LLM-empowered Visual Instruction Tuning

Zhihao Li^{a,*}, Yao Du^{b,***}, Yang Liu^b, Yan Zhang^c, Yufang Liu^d, Mengdi Zhang^b, Xunliang Cai^b, Charles Ling^a and Boyu Wang^{a,***}

^aDepartment of Computer Science, Western University, London, N6A 5B7, Ontario, Canada

^bMeituan Inc., Beijing, 100102, China

^cDepartment of Automation, Tsinghua University, Beijing, 100084, China

^dSchool of Computer Science and Technology, East China Normal University, Shanghai, 200062, China

ARTICLE INFO

Keywords:

Large Language Models
Visual Perception
Image Processing
Multi-modal Learning
Visual Instruction Tuning

ABSTRACT

Multi-modal Large Language Models (MLLMs) have advanced greatly in general tasks. However, they still face challenges in geometric reasoning, a task that requires synergistic integration of visual recognition proficiency and complex reasoning strength. Existing MLLMs prioritize optimizing the LLM backbone to enhance problem-solving capabilities, while rarely emphasizing improvements in discerning visual elements. However, we reveal that MLLMs suffer from severe visual perception deficiencies, including inaccurate geometric comprehension and severe visual hallucinations, which constrain their reasoning performance. To address this issue, we revisit geometric reasoning through a visual-centric lens that highlights the role of visual perception. To achieve this, we propose **EAGLE**, a novel coarse-to-fine visual enhancement framework that progressively leverages LLMs' guidance to improve perception proficiency. Specifically, given the substantial disparity between geometric diagrams and natural images, we first introduce **Geometric Knowledge Injection**. This process explores fundamental knowledge from diagram-caption data to enhance recognition capabilities and improve geometry-language alignments. Then, recognizing that different elements contribute unequally in the reasoning process, we introduce **Geometric Knowledge Refinement**. This stage leverages LLM-driven chain-of-thought solutions to guide the vision encoder in adaptively prioritizing key elements, fostering a synergistic interplay between visual comprehension and mathematical reasoning. Finally, we develop EAGLE, a geometry expert with strong perception and reasoning capabilities. Extensive experiments demonstrate its effectiveness on three popular benchmarks.

1. Introduction

Large Language Models (LLMs) have demonstrated remarkable performance across a variety of tasks (Zou et al., 2025; Liao et al., 2025). Latest LLMs even exhibit human-level reasoning capabilities in complicated tasks such as mathematical problem-solving (Imani et al., 2023; Zhu et al., 2024b) and code generation (Sun et al., 2024; Chai et al., 2025). These studies mainly focus on textual contexts, while multi-modal mathematical problems (Zheng et al., 2024; Gao et al., 2025) that require extra visual comprehension proficiency remain relatively underexplored. Due to the intrinsic limitation of LLMs in *visual perception*, they are not well-suited for solving such problems. Consequently, Multi-modal Large Language Models (MLLMs), which extend LLMs by incorporating an additional vision encoder, have attracted substantial attention.

MLLMs have demonstrated strong performance on general multi-modal tasks (Xu et al., 2015; Antol et al., 2015). However, they still face challenges in complex reasoning.

In particular, Geometry Problem Solving (GPS), an inherently challenging task that requires the synergy of precise visual perception and rigorous mathematical deduction, has emerged as a valuable testbed. Recent works (Shi et al., 2024; Gao et al., 2025) have made preliminary efforts by fine-tuning LLMs on geometric data. However, these studies mainly focus on improving the reasoning capacity of the LLM backbone, largely overlooking the reliability of the visual comprehension, which is typically supported by the standard CLIP ViT (Radford et al., 2021). However, due to the substantial domain gap between CLIP's natural image pre-training and geometric diagrams, we reveal that CLIP's inadequate geometric recognition capability is another primary bottleneck, and our empirical analysis substantiates this deficiency. Specifically, as visualized in Figure 1 and Figure 2, CLIP fails to accurately identify fundamental elements (e.g., points, lines, angles). This perceptual ambiguity propagates to the language model, leading to severe hallucinations and inaccurate descriptions. Such inadequacies limit MLLMs' problem-solving capability, underscoring the urgency to adapt vision encoders to the geometric domain.

Conventional visual optimization strategies typically pretrain the vision encoder in isolation from the overall MLLM architecture. For example, MAVIS (Zhang et al., 2025b) fine-tunes the CLIP ViT using geometric image-caption pairs, employing the CLIP text encoder as a proxy for supervision. While this paradigm enhances basic geometric

*Work done during an internship at Meituan.

**Corresponding authors.

✉ zli3446@uwo.ca (Z. Li); duyao10@meituan.com (Y. Du); liuyang509@meituan.com (Y. Liu); yzhang1995@mail.tsinghua.edu.cn (Y. Zhang); yfliu.antnlp@gmail.com (Y. Liu); zhangmengdi02@meituan.com (M. Zhang); caixunliang@meituan.com (X. Cai); charles.ling@uwo.ca (C. Ling); bwang@csd.uwo.ca (B. Wang)

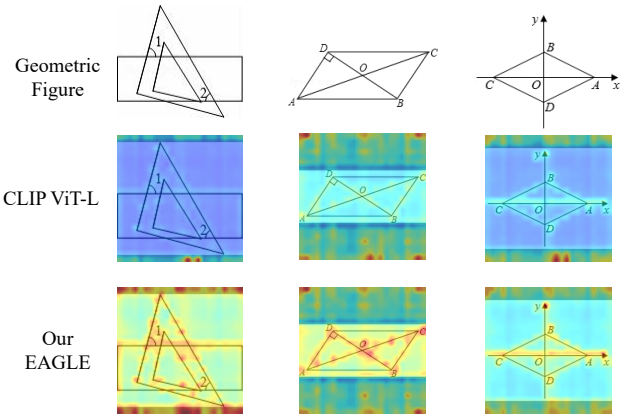


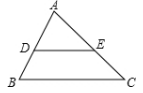
Figure 1: Comparison of attention maps between CLIP ViT and EAGLE. Regions highlighted with warm colors denote areas with higher model attention, whereas regions with cold colors indicate lower attention. It can be seen that CLIP ViT struggles to capture geometric shapes.

perception, the absence of the target LLM during visual optimization risks introducing feature misalignment. Moreover, prior studies (Shi et al., 2024; Gao et al., 2025) overlook the nuanced visual demands in reasoning tasks, where distinct geometric components play varying roles in the problem-solving process. Consequently, MLLMs must learn to prioritize visual elements according to their relevance to the solution path, an ability that can only be cultivated by leveraging the high-level reasoning rationale from the LLM. Consequently, we contend that solving the above challenges necessitates continual semantic guidance from LLMs, which highlights the need for a geometry-centered framework that facilitates dynamic interaction between visual perception and mathematical reasoning.

To address the aforementioned issue, we propose **EAGLE**, a coarse-to-fine visual enhancement framework that **ElevAtes Geometric reasoning through LLM-Empowered visual instruction tuning**. The core idea is to progressively inject geometric expertise into the vision encoder with continual guidance from LLMs. Our training pipeline consists of two stages: **Geometric Knowledge Injection** and **Geometric Knowledge Refinement**. In the first stage, we enhance visual understanding of basic geometric elements using diagram-caption data. This process not only equips the vision encoder with fundamental geometric knowledge but also establishes adaptive geometry-language alignments with the LLM backbone. Moreover, recognizing that different elements play inherently unequal roles in deriving solutions, we further refine the vision encoder in the second stage to capture critical features. This subtle optimization is guided by LLM’s step-by-step problem-solving solutions. Specifically, we leverage question-answer data with chain-of-thought (CoT) rationales. During this refinement, the vision encoder undergoes fine-grained adjustments to distinguish key visual cues essential for reasoning. Note that generic visual optimization like LLaVA-NeXT (Li et al.,



Please describe this geometric image in detail.



The image features a triangle with a square inside it, forming a unique shape. The triangle is composed of three sides, with one side being longer than the other two. The square is positioned within the triangle, with its corners meeting the triangle's sides. The triangle is also accompanied by a smaller triangle, which is located at the top left corner of the main triangle. The image is presented in black and white, giving it a classic and elegant appearance.



The figure depicts a diagram of a triangle, where the base BC is 10cm, and the height of the triangle is 5cm. The area of triangle ABC is 20cm². The area of triangle ADE is 10cm².



The diagram shows a triangle ABC with vertices A, B, and C. Point D lies on the line segment AB, and point E lies on the line segment AC. A line DE is drawn parallel to the line segment BC.



Figure 2: Comparison of the geometric caption performance. EAGLE exhibits remarkable geometric perception capability (green background) while LLaVA-1.5 and G-LLaVA face severe visual hallucinations (red background).

2024) and ShareGPT4V (Chen et al., 2025) straightforwardly unlocks the vision encoder without considering domain gaps. However, our ablation studies demonstrate that such simplistic strategies yield only marginal gains or even induce performance degradation. Finally, we present EAGLE, a 7B-scale specialist that excels in geometric perception and reasoning. Our contributions are as follows:

- We unveil a critical visual perception bottleneck in MLLMs for geometry problem solving, substantiated through in-depth attention map visualizations and evaluations of geometric captioning capabilities.
- We propose a coarse-to-fine visual enhancement framework that progressively enhances perception proficiency through LLM guidance. Specifically, the Geometric Knowledge Injection stage enables the vision encoder to acquire fundamental geometric knowledge and facilitates geometry-language alignment. Subsequently, the Geometric Knowledge Refinement stage leverages LLM-driven Chain-of-Thought (CoT) rationales to refine the vision encoder, prioritizing reasoning-critical geometric elements.
- We develop the geometric specialist model EAGLE, which exhibits competitive performance on popular benchmarks with only 7B parameters. Extensive quantitative and qualitative experiments demonstrate the effectiveness of our model.

The remainder of this paper is organized as follows. Section 2 analyzes the visual perception deficiency. Section 3 elaborates on the proposed visual enhancement framework. Section 4 presents extensive experiments. Section 5 discusses potential applications. Finally, Section 6 reviews related work, and Section 7 concludes the paper.

2. Observation on Visual Inadequacy

Existing MLLMs mostly utilize a fixed CLIP ViT to interpret geometric diagrams and then perform reasoning. The feasibility of this paradigm heavily depends on the reliability of the vision encoder. However, due to the disparity between CLIP’s pre-training images and geometric figures, it struggles to capture geometric elements accurately. In this section, we make pioneering efforts to investigate the geometric perception performance of current MLLMs and reveal their visual deficiency in geometric domains. Specifically, we visualize the attention map and examine MLLM’s performance in generating geometric-relevant captions, and we observe two noticeable phenomena as follows:

- **Insufficient perception of geometric elements.** As shown in Figure 1, we observe that CLIP struggles to capture critical elements within geometric diagrams effectively. Specifically, it fails to focus on general geometry elements (e.g., lines, dots, angles) and corresponding marks (e.g., angle 1, vertex A). Such observation reveals that integrating a frozen vision encoder into MLLMs is inadequate to capture essential visual details and provide satisfactory geometric comprehension, which naturally hinders the geometric problem-solving capability of MLLMs.
- **Severe visual geometric hallucinations.** Multi-modal hallucinations often entail the generation of descriptions for non-existent elements (Zhang et al., 2024). Similarly, MLLMs also encounter hallucinations when processing geometric diagrams. As illustrated in Figure 2, both the generalist model LLaVA-1.5 (Liu et al., 2024a) and the geometry-specialist model G-LLaVA (Gao et al., 2025) generate non-existent objects and fail to describe the spatial relationships among existing elements accurately. Notably, this limitation persists despite G-LLaVA having optimized its LLM backbone with geometry datasets. Such hallucinations result in unreliable or even erroneous geometric comprehension, thereby significantly impeding the subsequent reasoning process. Consequently, these findings further underscore the necessity of enhancing MLLMs’ vision encoder in specific geometric domains to ensure reliable visual comprehension.

3. Method

In this section, we elaborate on the two-stage coarse-to-fine visual enhancement framework in detail, as shown in Figure 3. Given that reasoning is more challenging than general tasks (Zhang et al., 2025a; Ke et al., 2025), we first learn to recognize fundamental elements (groundwork) and then dynamically prioritize them during reasoning (reasoning-specific refinement), enabling progressive adaptation to geometric domains. Both stages perform visual optimization under guidance from LLMs, fostering a synergistic interaction between the vision encoder and the LLM backbone.

3.1. Stage 1: Geometric Knowledge Injection

As discussed before, the CLIP ViT equipped by MLLMs exhibits severe deficiencies due to the domain gap between geometric and natural images. To mitigate this issue, we focus on injecting fundamental geometric knowledge (e.g., elements, shapes, and correlations) into the vision encoder. The goal is to adapt the vision encoder to geometric domains and establish groundwork for more advanced reasoning. Specifically, we utilize 60K diagram-caption pairs to fine-tune ViT in an end-to-end manner, with the CLIP ViT perceiving images and the frozen LLM interpreting textual descriptions as guidance. We also optimize the projector between two unimodal encoders to foster adaptive geometry-language alignments. It is noteworthy that our Geometric Knowledge Injection differs from existing fine-tuning strategies that decouple ViT from MLLMs and optimize it separately (Zhang et al., 2025b), which may introduce extra discrepancies when aligning with LLMs. Differently, we integrate visual optimization into an end-to-end MLLM training pipeline. This process fine-tunes ViT and fosters geometric vision-language alignment simultaneously, which equips the model with superior geometric expertise. To summarize, we optimize the vision encoder and the cross-modal projector during this stage. The LLM backbone is kept frozen to maintain consistent textual guidance.

3.2. Stage 2: Geometric Knowledge Refinement

After the knowledge injection stage, the vision encoder is equipped with fundamental geometric knowledge and is capable of describing geometric diagrams reliably. However, geometric reasoning poses greater challenges than captioning tasks, as it not only demands precise recognition but also requires the model to prioritize elements that are critical for correct reasoning. To enhance this capability, we leverage the LLM-driven step-by-step problem-solving process to further refine the vision encoder. This process is also achieved in an end-to-end MLLM training pipeline, where 110K question-answer pairs with detailed solution steps are employed for visual instruction tuning. Specifically, we incorporate LoRA (Hu et al., 2022) modules into the vision encoder to capture key visual cues during reasoning, while we keep the main body of the ViT frozen to maintain its prior geometric perceptual knowledge. Moreover, we unfreeze the LLM backbone to improve its reasoning strength, which continually guides the refinement of the vision encoder. In this stage, as the LLM absorbs knowledge from CoT rationales, the LoRA-based vision encoder focuses on capturing key geometric clues and discovers their inter-correlations, promoting in-depth geometric comprehension. We note that standard instruction tuning (Shi et al., 2024; Gao et al., 2025) typically focuses on improving LLMs with a frozen ViT, while our Knowledge Refinement surpasses them by leveraging CoT solutions to reveal key elements that ViT should prioritize, leading to superior geometric comprehension. To summarize, we employ LoRA for the vision encoder while keeping the cross-modal projector and the LLM backbone trainable during this stage.

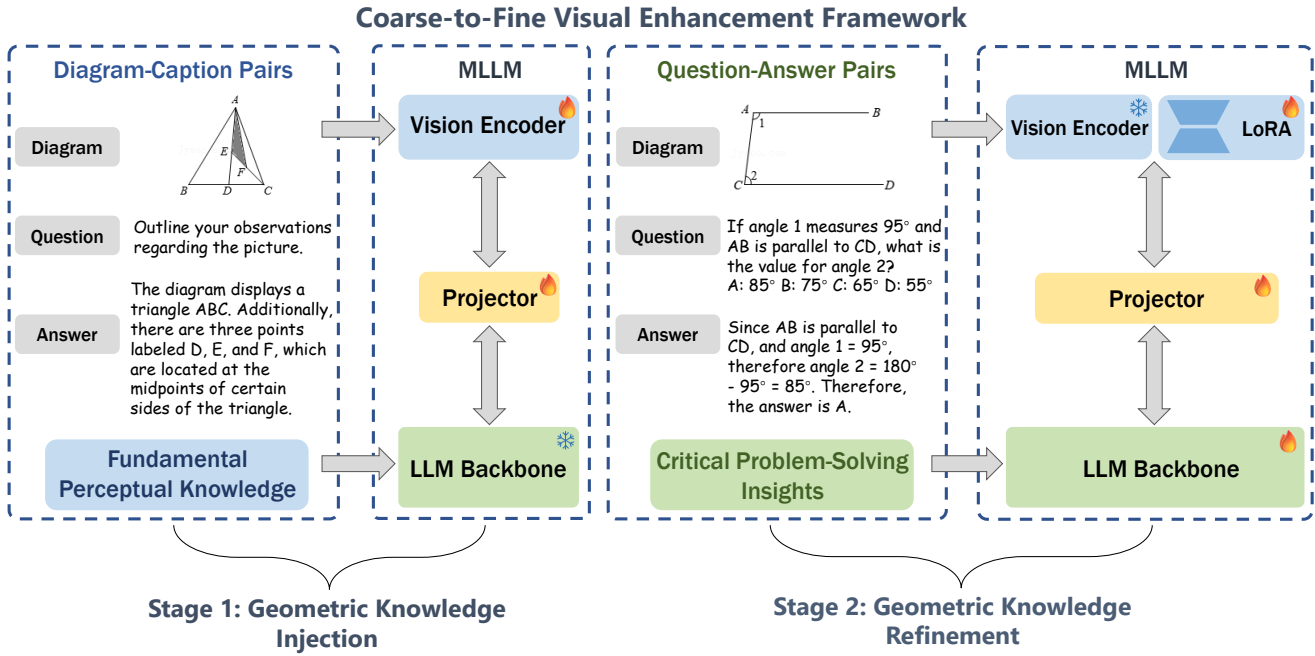


Figure 3: The overview of our proposed coarse-to-fine visual enhancement framework. During Geometric Knowledge Injection, fundamental geometric knowledge is extracted from diagram-caption data, enhancing the recognition capabilities of the vision encoder. During Geometric Knowledge Refinement, critical problem-solving insights are derived from LLM-driven step-by-step question-answer pairs, further refining the vision encoder to prioritize essential geometric elements during reasoning.

3.3. Model Training

To ensure consistency and reduce potential biases in the geometry-centered visual enhancement framework, we employ end-to-end training at both stages rather than optimizing the vision encoder separately. We utilize an auto-regressive language modeling loss as the training objective. Specifically, to generate the t^{th} token, the geometry diagram I , the input sentence S_{in} , and the predicted tokens up to the t^{th} step are fed into our model \mathcal{F} for next-token predictions. This process can be formulated as follows:

$$\mathcal{L}(S_{tar}, S_{in}, I) = - \sum_{t=1}^l \log p \left[S_{tar}^t \middle| \mathcal{F}(S_{tar}^{(<t)}, S_{in}, I) \right], \quad (1)$$

where S_{tar} denotes the target sentence, l denotes the length.

4. Experiment

In this section, we present a comprehensive evaluation of EAGLE through extensive experiments on three widely recognized benchmarks. Beyond standard performance metrics, we conduct in-depth ablation studies to rigorously verify the individual contribution and efficacy of each proposed training strategy. Finally, we provide detailed qualitative visualizations and specific case studies, which further demonstrate the superior capabilities of the proposed coarse-to-fine visual enhancement framework in geometric perception and complex problem-solving.

Table 1

Hyper-parameter settings. “Geo-KI” and “Geo-KR” indicate Geometric Knowledge Injection and Geometric Knowledge Refinement, respectively.

	Geo-KI	Geo-KR
Batch Size	48	
Learning Rate (LR)	1e-5	3e-5
LR Schedule	cosine decay	
LR Warmup Ratio	0.03	
Epoch	1	2
Optimizer	AdamW	
LoRA Alpha	–	16
LoRA Rank	–	64
LoRA Dropout	–	0.05

4.1. Experiment Settings

Datasets. We utilize the geometry-specific Geo170K dataset introduced by G-LLaVA (Gao et al., 2025) to train our model. Geo170K is constructed utilizing the training sets of GeoQA+ (Cao and Xiao, 2022) and Geometry3K (Lu et al., 2021), which consists of two parts: 60K examples of geometric alignment data primarily in the form of image-caption pairs, and 110K examples of geometric question-answer data with detailed CoT rationales.

Implementation Details. We develop EAGLE with the LLaVA-1.5 architecture (Liu et al., 2024a), which comprises a CLIP ViT-L/14 (Radford et al., 2021) as the vision encoder and a 7B Vicuna-1.5 (Chiang et al., 2023) as the LLM backbone. We employ a two-layer MLP as the cross-modal projector to connect the vision encoder and the base LLM.

Table 2

Comparison on the GeoQA benchmark.

Methods	LLM Backbone	LLM Size	Accuracy
<i>Heuristics Baselines</i>			
Random Chance	-	-	25.0
Frequent	-	-	32.1
<i>Conventional Models</i>			
Geoformer (Chen et al., 2022)	-	-	46.8
UniMath (Liang et al., 2023)	-	-	50.0
<i>General MLLMs</i>			
mPLUG-Owl2 (Ye et al., 2024a)	LLaMA-2	7B	15.7
ShareGPT4V (Chen et al., 2025)	Vicuna-1.5	7B	16.2
LLaVA-1.5 (Liu et al., 2024a)	Vicuna-1.5	7B	21.1
LLaVA-1.5 (Liu et al., 2024a)	Vicuna-1.5	13B	23.2
LLaVA-NeXT (Li et al., 2024)	LLaMA-3	8B	33.9
Qwen2-VL (Yang et al., 2024)	Qwen2	7B	46.2
Qwen2.5-VL (Yang et al., 2025)	Qwen2.5	3B	56.8
InternVL2.5 (Chen et al., 2024)	QLLaMA	8B	58.1
GPT-4o (Hurst et al., 2024)	-	-	61.4
<i>Mathematical MLLMs</i>			
Math-LLaVA (Shi et al., 2024)	Vicuna-1.5	13B	47.8
Math-PUMA (Zhuang et al., 2025)	DeepSeek-Math	7B	61.8
Math-PUMA (Zhuang et al., 2025)	Qwen2	7B	63.6
G-LLaVA (Gao et al., 2025)	LLaMA-2	7B	64.2
InternLM-XC2 (Dong et al., 2024)	InternLM2	7B	66.4
MAVIS w/o DPO (Zhang et al., 2025b)	MAmmoTH-2	7B	66.7
EAGLE	Vicuna-1.5	7B	67.1

The input image resolution is set to 336 by 336 pixels. The detailed training hyper-parameter settings are presented in Table 1. Specifically, to avoid overfitting, we follow G-LLaVA (Gao et al., 2025) to train EAGLE for one epoch in the geometric knowledge injection stage and two epochs in the geometric knowledge refinement stage. We employ the AdamW optimizer (Loshchilov and Hutter, 2019) during the training process. The learning rate is set to $1e^{-5}$ and $3e^{-5}$ on each stage with a cosine decay learning rate scheduler. All experiments are conducted with eight NVIDIA A100 GPUs. **Evaluation and Metrics.** We evaluate our model on three popular benchmarks, namely GeoQA (Chen et al., 2021), MathVista (Lu et al., 2024b), and We-Math (Qiao et al., 2025). GeoQA is a commonly used geometry dataset that mainly focuses on plane geometry. MathVista encompasses various mathematical tasks that require visual comprehension, where we select the Geometry Problem Solving (GPS) task within the MathVista testmini subset for evaluation. We-Math explores the underlying problem-solving principles during the reasoning process beyond performance. All models are assessed in a zero-shot setting, where top-1 accuracy is adopted as the evaluation metric. Our model is specifically prompted to generate responses in a fixed format, and the predicted answers are automatically extracted via a regular expression.

4.2. Results and Analyses.

Comparisons on GeoQA. As shown in Table 2, EAGLE clearly outperforms mainstream MLLMs on GeoQA.

Specifically, EAGLE achieves notable 2.9% improvements compared with G-LLaVA (Gao et al., 2025), demonstrating the advancement of our coarse-to-fine visual enhancement, which endows the MLLM with collaborative geometric perception and reasoning strength. Moreover, EAGLE surpasses contemporary mathematical-centric approaches, such as Math-PUMA (Zhuang et al., 2025) (trained on 996K multimodal mathematical data) and MAVIS w/o DPO (Zhang et al., 2025b) (trained on more than 1.4M mathematical examples), despite being trained on a substantially smaller dataset comprising only 170K examples. The superior performance of EAGLE with less mathematical training data further substantiates the effectiveness in mitigating the geometric perception bottlenecks of MLLMs.

Comparisons on MathVista. As shown in Table 3, EAGLE achieves 54.3% accuracy in Geometry Problem Solving and outperforms GPT-4V by 3.8% on the testmini split of MathVista. Compared with other 7B models, it also exhibits superior performance. For example, EAGLE exceeds its baseline model LLaVA-1.5-7B with a clear margin of 37% and the seminal G-LLaVA-7B model by 0.9%. Notably, EAGLE also surpasses larger 13B models like SPHINX-V1 (Lin et al., 2023) and LLaVAR (Zhang et al., 2023). These results demonstrate the superiority of enhancing the vision encoder and the effectiveness of leveraging LLMs to guide ViT optimization through a tailored coarse-to-fine strategy, which directs EAGLE to recognize and prioritize key geometric elements in reasoning tasks. By harnessing

Table 3

Comparison on testmini set of the MathVista benchmark for Geometry Problem Solving.

Methods	LLM Backbone	LLM Size	Accuracy
	<i>Heuristics Baselines</i>		
Random Chance	-	-	21.6
Frequent	-	-	34.1
Human	-	-	48.4
<i>General MLLMs</i>			
LLaVA-1.5 (Liu et al., 2024a)	Vicuna-1.5	7B	17.3
LLaVA-1.5 (Liu et al., 2024a)	Vicuna-1.5	13B	18.8
InstructBLIP (Dai et al., 2023)	Vicuna	7B	20.7
ShareGPT4V (Chen et al., 2025)	Vicuna-1.5	7B	22.1
SPHINX-V1 (Lin et al., 2023)	LLaMA-2	13B	23.1
mPLUG-Owl (Ye et al., 2023)	LLaMA	7B	23.6
Genimi 1.0 Nano2 (Team et al., 2023)	-	-	23.6
LLaVA-NeXT (Li et al., 2024)	LLaMA-3	8B	25.0
LLaVAR (Zhang et al., 2023)	Vicuna	13B	25.0
MiniGPT4 (Zhu et al., 2024a)	LLaMA-2	7B	26.0
Qwen-VL-Plus (Bai et al., 2023)	Qwen	7B	38.5
Gemini 1.0 pro (Team et al., 2023)	-	-	40.4
Qwen2.5-VL (Yang et al., 2025)	Qwen2.5	3B	42.2
Qwen2-VL (Yang et al., 2024)	Qwen2	7B	49.0
GPT-4V (OpenAI, 2023)	-	-	50.5
<i>Mathematical MLLMs</i>			
Deepseek-VL (Lu et al., 2024a)	DeepSeek-LLM	7B	28.4
VCAR (Jia et al., 2024)	Vicuna-1.5	7B	34.6
Math-PUMA (Zhuang et al., 2025)	DeepSeek-Math	7B	39.9
Qwen2-VL (Wang et al., 2024a)	Qwen2	7B	40.9
Math-PUMA (Zhuang et al., 2025)	Qwen2	7B	48.1
G-LLaVA (Gao et al., 2025)	LLaMA-2	7B	53.4
EAGLE	Vicuna-1.5	7B	54.3

advanced perceptual capabilities, our model achieves exceptional proficiency in solving complex geometric problems.

Comparisons on We-Math. To investigate the underlying principles of mathematical reasoning, we employ the We-Math benchmark with its granular four-dimensional metrics. As presented in Table 4, EAGLE outperforms DeepSeek-VL-7B (Lu et al., 2024a) by a clear margin across nearly all metrics. Moreover, it also exhibits superior performance against G-LLaVA (Gao et al., 2025) in the average loose score while maintaining parity under the rigorous strict criterion. Crucially, EAGLE attains the highest score in Complete Mastery (CM) under the loose setting (20.57%), indicating a superior capability in capturing genuine logical dependencies. Collectively, these results demonstrate that our coarse-to-fine enhancement strategy effectively boosts reasoning reliability across diverse evaluation standards.

4.3. Further Analysis

Analysis of Geometric Knowledge Injection. Geometric Knowledge Injection leverages diagram-caption pairs to equip the MLLM with fundamental geometric knowledge, laying the groundwork for subsequent prioritization on key elements. To rigorously validate its necessity, we systematically exclude it from the training pipeline and assess its impact on final performance, as shown in Table 5. We observe that Methods 1–3 consistently underperform

EAGLE, highlighting the critical role of knowledge injection in acquiring basic geometric expertise.

Analysis of Geometric Knowledge Refinement. We also investigate the impact of CoT-guided Knowledge Refinement, as presented in Table 5. Notably, Methods 1 to 3 demonstrate performance comparable to or exceeding that of the baseline G-LLaVA 7B solely via Geometric Knowledge Refinement, highlighting the effectiveness of leveraging CoT solutions to acquire visual perception knowledge. This process enables the LLM to progressively learn how to solve geometric problems step by step, while the vision encoder complements this by aligning its focus with the LLM’s reasoning trajectory and emphasizing critical visual details. We argue that this synergistic interplay is pivotal for addressing geometric problems, thereby outperforming G-LLaVA, even in the absence of explicit diagram-caption alignments.

4.4. Ablation Study

Different Strategies for Knowledge Injection. As shown in Table 6, we conduct comparative experiments to investigate different visual enhancement strategies for Knowledge Injection. Comparing EAGLE with Methods 1 and 2, we observe that fine-tuning the entire vision encoder in this stage leads to superior results. We explain that although the CLIP ViT has been trained on an extensive corpus of natural images,

Table 4

Comparison on the We-Math testmini set with four-dimensional metrics (IK: Insufficient Knowledge, IG: Inadequate Generalization, CM: Complete Mastery, RM: Rote Memorization) of two criteria (Loose and Strict). Avg. denotes the average score. The best and second-best scores in each category are marked in **bold** and underlined, respectively.

Methods	Avg. (Loose)↑	IK↓	IG↓	CM↑	RM↓	Avg. (Strict)↑	IK↓	IG↓	CM↑	RM↓
DeepSeek-VL-7B	20.95	69.14	4.57	18.67	28.99	<u>6.29</u>	69.14	4.57	4.00	84.78
G-LLaVA	<u>22.29</u>	64.19	4.57	<u>20.00</u>	35.98	6.48	64.19	4.57	<u>4.19</u>	86.59
EAGLE	22.86	<u>66.10</u>	4.57	20.57	29.87	6.48	<u>66.10</u>	4.57	4.19	<u>85.71</u>

Table 5

Further analysis of the training pipeline with different visual enhancement strategies. “Geo-KI” and “Geo-KR” indicate Geometric Knowledge Injection and Geometric Knowledge Refinement, respectively. “FFT” denotes Full Fine-tuning. Results are obtained on the GeoQA benchmark.

Methods	Geo-KI	Geo-KR	Accuracy
G-LLaVA	Freeze	Freeze	64.2
1	-	LoRA	63.8
2	-	FFT	64.3
3	-	Freeze	64.6
EAGLE	FFT	LoRA	67.1

its limited exposure to geometry diagrams hinders its recognition and comprehension performance. Consequently, fully fine-tuning the vision encoder significantly facilitates the geometry-centered visual augmentation and establishes the groundwork for a deeper reasoning process.

Different Strategies for Knowledge Refinement. Knowledge Refinement aims to guide visual optimization with step-by-step problem-solving expertise. For deeper comprehension, we evaluate various refining strategies, including fine-tuning the entire vision encoder, freezing the vision encoder, and incorporating additional LoRA modules. As shown in Table 6, EAGLE achieves superior performance by integrating LoRA modules, while fully fine-tuning (Method 3) leads to unsatisfactory results, even poorer than freezing the visual backbone (Method 4). We argue that fine-tuning the entire ViT in this stage may disrupt its prior knowledge acquired from Geometric Knowledge Injection, highlighting the efficacy of our delicate refining strategy in capturing key elements while maintaining comprehensive perception.

Performance with a frozen LLM backbone. We further demonstrate the efficacy of coarse-to-fine visual enhancement by applying it while freezing the core LLM. Specifically, we freeze the LLM backbone throughout the training pipeline, updating only the vision encoder and projector in the same manner as before. As shown in Table 7, even though EAGLE* relies entirely on the original reasoning capabilities of the frozen LLM and conducts reasoning without new geometric-specific problem-solving expertise, it still achieves a clear 10.3% improvement over the baseline LLaVA-1.5-7B. This result directly confirms that clearer visual perception alone can significantly boost geometric problem-solving, thereby reinforcing our identification of

Table 6

Impact of different training strategies on the vision encoder. During the Geo-KI stage, the projector remains trainable, while the LLM backbone is kept frozen. In the Geo-KR stage, both the projector and the LLM are set to be trainable. Results are obtained on the GeoQA benchmark.

Methods	Geo-KI	Geo-KR	Accuracy
1	Freeze	LoRA	62.3
2	-	LoRA	65.1
3	-	FFT	64.2
4	-	Freeze	66.1
EAGLE	FFT	LoRA	67.1

Table 7

Impact of LLM during the Knowledge Refinement stage. Results are obtained on the GeoQA benchmark.

Methods	Vision Encoder	LLM	Accuracy
LLaVA-1.5-7B	-	-	21.1
LLaVA-1.5-13B	-	-	23.2
EAGLE*	LoRA	Freeze	31.4
EAGLE	LoRA	FFT	67.1

the visual bottleneck and demonstrating the pivotal efficacy of the proposed visual enhancement framework.

4.5. Qualitative Analysis

More Attention Map Visualizations. We provide additional qualitative evidence through attention map visualizations of the vision encoder, further underscoring the superior perceptual capability of EAGLE over baseline LLMs that utilize a frozen CLIP ViT. As illustrated in Figure 4, the original CLIP ViT struggles to discern fine-grained fundamental geometric structures, such as vertices, angles, and outlines. In contrast, empowered by the proposed coarse-to-fine visual enhancement framework, EAGLE effectively mitigates this limitation and precisely localizes these geometric elements. These results demonstrate that our method successfully establishes a well-grounded visual foundation for subsequent rigorous reasoning.

Case Studies on GeoQA. As illustrated in Figure 5, we conduct qualitative comparisons between EAGLE and the geometric specialist model, G-LLaVA, on the GeoQA test set. Our analysis reveals that G-LLaVA has severe geometric hallucinations, which frequently fabricates spurious

Geometric Figure

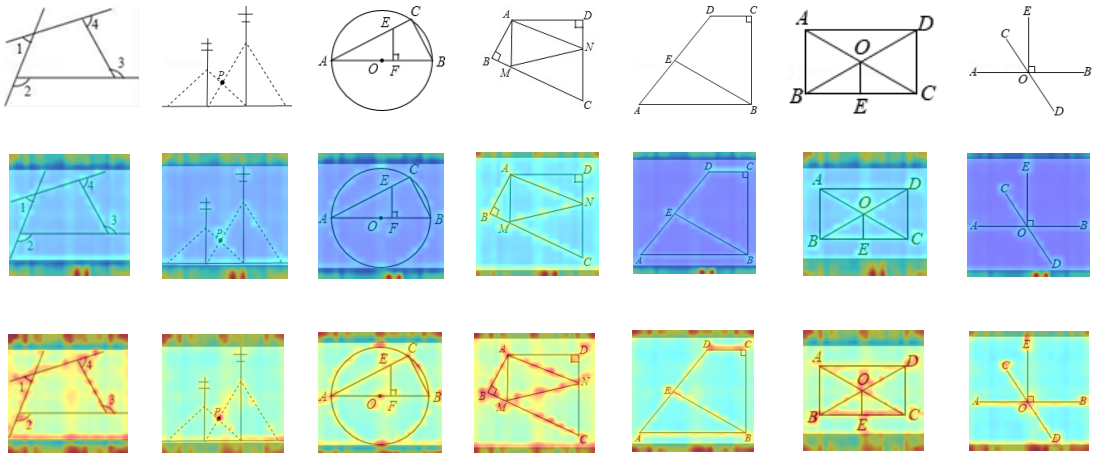
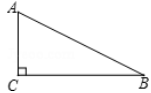


Figure 4: More attention map visualizations between CLIP ViT and EAGLE.

Question: As shown in the figure, in triangle ABC, angle C = 90.0, AC = 1.0, BC = 2.0, then the value of cos B is ()
 Choices: A: $\sqrt{5}/5$ B: $2\sqrt{5}/5$ C:1/2 D:2

Answer: B



G-LLaVA: Solution: Given that in triangle ABC, angle C is 90°, $AB = \sqrt{AC^2 + BC^2} = \sqrt{1^2 + 2^2} = \sqrt{5}$. Therefore, $\cos B = AC/AB = 1/\sqrt{5} = \sqrt{5}/5$. Therefore, the answer is A.

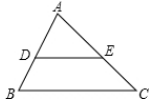


EAGLE: Solution: $\cos B = BC/AB = 2/\sqrt{5} = 2\sqrt{5}/5$. Therefore, the answer is B.

Question: As shown in the figure, in triangle ABC, it is known that angle A = 80.0, angle B = 60.0, DE parallel BC, then the size of angle CED is ()

Choices: A:40° B:60° C:120° D:140°

Answer: D



G-LLaVA: Solution: Since angle A is 80 degrees and angle B is 60 degrees, therefore angle ACB is equal to 180 degrees minus angle A minus angle B, which is equal to 180 degrees minus 80 degrees minus 60 degrees, which is equal to 40 degrees. Since DE is parallel to BC, angle CED is equal to angle ACB, which is 40 degrees. Therefore, the answer is option A.

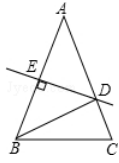


EAGLE: Solution: By using the fact that the sum of the interior angles of a triangle is 180°, we can find that angle C = 180° - angle A - angle B = 180° - 80° - 60° = 40°. Since DE is parallel to BC, we can conclude that angle CED = 180° - angle C = 180° - 40° = 140°. Therefore, the answer is D.

Question: As shown in the figure, in triangle ABC, AB = AC, angle A = 36.0, the perpendicular bisector of AB intersects AC at D, and intersects AB at E, then the degree of angle BDC is ()

Choices: A:72° B:36° C:60° D:82°

Answer: A



G-LLaVA: Solution: Because AB = AC and angle A = 36°, therefore angle C = 72°. Since DE is perpendicular bisector of AB, AE = BE, and angle B = angle A = 36°. Therefore, angle BDC = angle C + angle B = 72° + 36° = 108°. Hence, the answer is D.

EAGLE: Solution: Since in triangle ABC, AB=AC, angle A=36°. Therefore, angle ABC=72°. Since the perpendicular bisector of AB intersects AC at D and intersects AB at E. Therefore, DB=DA. Therefore, angle DBA=angle A=36°. Therefore, angle BDC=72°. Therefore, option A is correct.

Figure 5: Comparison of the geometric problem-solving capability between EAGLE and G-LLaVA on the GeoQA test set. Red background indicates incorrect reasoning, whereas green background highlights correct problem-solving processes.

geometric attributes (e.g., non-existent height and angle values) and constructs flawed problem-solving processes that lead to incorrect conclusions. Specifically, in the first case, G-LLaVA exhibits a fundamental disconnect between visual perception and mathematical formulation by incorrectly computing the cosine of angle B as $\cos B = AC/AB$, failing to effectively integrate symbolic visual perception into mathematical reasoning. In the second case, G-LLaVA generates inaccurate diagram descriptions (as previously noted in Figure 2), which further compromises its reasoning process and results in incorrect answers. In contrast, EAGLE

demonstrates effective synergies between vision perception and mathematical reasoning. It not only generates precise and detailed descriptions of geometric diagrams but also effectively identifies and prioritizes critical geometric elements, which enables reliable step-by-step solutions.

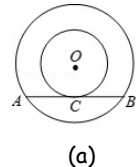
Case Studies on MathVista. We also provide reasoning cases from the testmini set of MathVista regarding Geometry Problem Solving. As shown in Figure 6, EAGLE effectively addresses geometric problems of various types, including calculations of area, angle, length, and trigonometric functions. Notably, in Figure 6 (a), EAGLE even demonstrates



Question: As shown in the figure, in the two concentric circles, the chord AB of the great circle is tangent to the small circle at point C. If $AB = 6.0$, the area of the ring is ()

Choices: A: 9π B: 6π C: 3π D: π

Answer: A



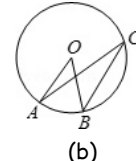
Solution: Connect OA and OC as shown in the figure. Since the chord AB of the larger circle is tangent to the smaller circle at point C, we have OC perpendicular to AB. Therefore, $AC=BC=1/2AB=3$. In right triangle OAC, $OA^2-OC^2=AC^2=3^2=9$. Thus, the area of the annulus in the figure is $S_{\text{larger circle}}-S_{\text{smaller circle}}=\pi\cdot OA^2-\pi\cdot OC^2=\pi(OA^2-OC^2)=9\pi$. Therefore, the answer is A.



Question: As shown in the figure, point O is the center of $\odot O$, points A, B, and C are on $\odot O$, $AO \parallel BC$, $\angle AOB = 40.0$, then the degree of $\angle OAC$ is equal to ()

Choices: A: 40° B: 60° C: 50° D: 20°

Answer: D



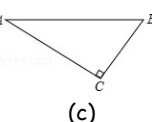
Solution: Since AO is parallel to BC , we have angle OAC = angle ACB . Additionally, both angle AOB and angle ACB are angles that are opposite to arc AB . Therefore, angle $ACB = 1/2$ angle $AOB = 20^\circ$. Hence, the measure of angle OAC is 20° . Therefore, the answer is D.



Question: As shown in the figure: In $\triangle ABC$, $\angle C = 90.0$, $AC = 8.0$, $AB = 10.0$, then the value of $\sin B$ is equal to ()

Choices: A: $\frac{3}{5}$ B: $\frac{4}{5}$ C: $\frac{3}{4}$ D: $\frac{4}{3}$

Answer: B



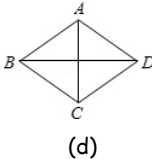
Solution: Since in right triangle ABC, angle $C = 90^\circ$, $AC = 8$, $AB = 10$, therefore $\sin B = AC/AB = 8/10 = 4/5$. Thus, the answer is B.



Question: As shown in the figure, in the diamond ABCD, two diagonal lines $AC = 12.0$, $BD = 16.0$, then the edge length of this diamond is ()

Choices: A: 10 B: 8 C: 6 D: 5

Answer: A



Solution: Since the diagonals of a rhombus are perpendicular bisectors of each other, triangle AOB is a right-angled triangle. Also, we know that AC is equal to 2 times AO and BD is equal to 2 times BO . Therefore, AO is equal to 6 and BO is equal to 8. Consequently, AB can be found using the Pythagorean theorem, which gives us $\sqrt{(AO^2 + BO^2)} = 10$. Therefore, the correct answer is option A.

Figure 6: Geometric reasoning cases of EAGLE on the MathVista benchmark.

the proficiency to draw auxiliary lines to assist reasoning, such as connecting OA and OC to form the triangle OAC . These resolution processes further highlight the superior geometric recognition and problem-solving strength of our proposed model.

5. Potential for Broader Application

Our proposed coarse-to-fine visual enhancement framework is not specified in geometric problem-solving. It has the potential to boost the performance of MLLMs for various multi-modal tasks, as outlined below.

Extension to diverse mathematical domains. The visual inadequacy of CLIP is not confined to geometry but also manifests in other mathematical domains, including tabular structures and data visualizations. Such limitations substantially constrain the reasoning potential of MLLMs. Therefore, unfreezing the vision encoder to align with specific data distributions offers a generalizable solution for enhancing MLLM performance across diverse downstream tasks.

Robust supervision guided by LLMs. EAGLE demonstrates the efficacy of enhancing the vision encoder with LLMs through an end-to-end training pipeline. Consequently, leveraging the advanced linguistic encoding capabilities of LLMs offers a promising avenue for supervising diverse multi-modal tasks. For example, integrating an LLM-based text encoder into segmentation frameworks facilitates the precise interpretation of complex prompts and instructions, thereby enhancing model performance.

Novel optimization paradigm for cross-modal encoders. The success of EAGLE underscores the efficacy of the LLM-empowered visual enhancement framework. Given this, we consider the potential of leveraging LLMs to supervise cross-modal alignment. For example, different from conventional contrastive learning paradigms like CLIP, visual features extracted by a vanilla ViT can be directly projected into LLMs to synthesize corresponding descriptions. By optimizing the consistency between LLM-generated contents and ground-truth captions, the vision encoder is endowed with superior cross-modal representation capabilities.

6. Related Work

6.1. Multi-modal Large Language Models

Recent years have witnessed thriving developments for large language models (Bai et al., 2022; Touvron et al., 2023a,b), which display remarkable performance across various natural language processing tasks. Concurrently, many researchers attempt to harness the prowess of LLMs in diverse multi-modal scenarios, leading to the prosperity of multi-modal large language models (OpenAI, 2023; Liu et al., 2024b; Ye et al., 2024b; Nie et al., 2025; Zeng et al., 2025). Modern MLLMs typically comprise a vision encoder that extracts visual clues (e.g., CLIP (Radford et al., 2021)), a cross-modal projector that aligns visual and textual features, and a language foundation model that serves as the cognitive core (e.g., LLaMA (Touvron et al., 2023a)). In early studies, MLLMs primarily focus on conventional vision-language

tasks, as demonstrated by BLIP-2 (Li et al., 2023) and Mini-GPT4 (Zhu et al., 2024a). Recently, in light of the remarkable advancements achieved by LLMs in complex reasoning (Yu et al., 2024; Yuan et al., 2024), there has been a surge of research focusing on multi-modal reasoning (Wang et al., 2024b,c). For example, Zheng *et al.* (Zheng et al., 2023) devised a novel DDCoT prompting technique that decouples LLMs' reasoning and recognition capabilities, enabling the transfer of these advancements to multi-modal contexts. He *et al.* (He et al., 2024) proposed to improve the multi-modal CoT capability through latent space learning. Despite these significant achievements, we observe that MLLMs still face challenges in effectively addressing multi-modal mathematical problems involving geometric elements.

6.2. Geometry Problem Solving

Geometry problem solving (Jia et al., 2024; Zhuang et al., 2025; Gao et al., 2025; Xia et al., 2025) is a challenging reasoning task that requires MLLMs to possess proficiency in both visual perception and mathematical problem-solving. Given the rapid development of complex reasoning, many methods have achieved marked developments. For example, G-LLaVA (Gao et al., 2025) constructs a geometric dataset Geo170K and develops a geometric expert model. Math-LLaVA (Shi et al., 2024) develops a math-focused MLLM trained on a curated MathV360K dataset. These studies mainly focus on enhancing the LLMs' reasoning strength while neglecting the deficiency of visual recognition. Several methods have been proposed to mitigate this issue. For instance, MAVIS (Zhang et al., 2025b) developed a math-specific MAVIS-Caption dataset to fine-tune ViT through contrastive learning. However, these studies mostly conduct visual enhancement without LLMs' guidance, which hinders vision-language alignment and lacks exploration of their synergistic interplay. In contrast, we propose a coarse-to-fine visual enhancement framework that optimizes the vision encoder within an end-to-end MLLM training pipeline, promoting enhanced visual perception and reasoning strength simultaneously.

7. Conclusion

In this paper, we focus on mitigating the visual deficiency of MLLMs to enhance their geometry reasoning capabilities. We first reveal MLLMs' inadequate perception of geometric diagrams. Then, to address this, we propose a coarse-to-fine LLM-empowered visual enhancement framework and develop a geometric specialist model, EAGLE. Our approach is structured into two progressive stages: Geometric Knowledge Injection and Geometric Knowledge Refinement. In the first stage, EAGLE acquires fundamental geometric knowledge (e.g., dots, lines, angles) from diagram-caption data, enabling it to obtain precise geometric comprehension and establish reliable geometry-language alignment. In the second stage, EAGLE leverages LLM-driven step-by-step CoT solutions to guide the vision encoder in adaptively prioritizing key elements critical to the reasoning process. Through iterative optimization, the vision

encoder refines its recognition capability to capture essential details and transmit them seamlessly to the LLM backbone, fostering a dynamic interaction between visual perception and mathematical reasoning. Comprehensive evaluations on popular geometric benchmarks, along with in-depth ablation studies, demonstrate the effectiveness of EAGLE.

CRediT authorship contribution statement

Zhihao Li: Writing – original draft, Writing – review & editing, Methodology, Software. **Yao Du:** Formal Analysis, Writing – review & editing. **Yang Liu:** Conceptualization. **Yan Zhang:** Writing – review & editing. **Yufang Liu:** Conceptualization. **Mengdi Zhang:** Formal analysis. **Xunliang Cai:** Formal analysis. **Charles Ling:** Supervision. **Boyu Wang:** Writing – review & editing, Supervision.

Declaration of competing interest

The authors declare the following personal relationships, which may be considered as potential competing interests: Boyu Wang, given his role as Action Editor, had no involvement in the peer review of this article and had no access to information regarding its peer review. Full responsibility for the editorial process for this article was delegated to another journal editor. If there are other authors, they declare that they have no known competing financial interests or personal relationships that could have appeared to influence the work reported in this paper.

Acknowledgements

This work is supported by the Natural Sciences and Engineering Research Council of Canada (NSERC), Discovery Grants program.

Data availability

Data will be made available on request.

References

- Antol, S., Agrawal, A., Lu, J., Mitchell, M., Batra, D., Zitnick, C.L., Parikh, D., 2015. Vqa: Visual question answering, in: Proceedings of the IEEE International Conference on Computer Vision, pp. 2425–2433.
- Bai, J., Bai, S., Yang, S., Wang, S., Tan, S., Wang, P., Lin, J., Zhou, C., Zhou, J., 2023. Qwen-vl: A frontier large vision-language model with versatile abilities. arXiv preprint arXiv:2308.12966 .
- Bai, Y., Jones, A., Ndousse, K., Askell, A., Chen, A., DasSarma, N., Drain, D., Fort, S., Ganguli, D., Henighan, T., et al., 2022. Training a helpful and harmless assistant with reinforcement learning from human feedback. arXiv preprint arXiv:2204.05862 .
- Cao, J., Xiao, J., 2022. An augmented benchmark dataset for geometric question answering through dual parallel text encoding, in: Proceedings of the 29th International Conference on Computational Linguistics, pp. 1511–1520.
- Chai, L., Yang, J., Sun, T., Guo, H., Liu, J., Wang, B., Liang, X., Bai, J., Li, T., Peng, Q., et al., 2025. xcot: Cross-lingual instruction tuning for cross-lingual chain-of-thought reasoning, in: Proceedings of the AAAI Conference on Artificial Intelligence, pp. 23550–23558.

Chen, J., Li, T., Qin, J., Lu, P., Lin, L., Chen, C., Liang, X., 2022. Unigeo: Unifying geometry logical reasoning via reformulating mathematical expression, in: Proceedings of the 2022 Conference on Empirical Methods in Natural Language Processing, pp. 3313–3323.

Chen, J., Tang, J., Qin, J., Liang, X., Liu, L., Xing, E., Lin, L., 2021. Geoqa: A geometric question answering benchmark towards multimodal numerical reasoning, in: Findings of the Association for Computational Linguistics: ACLI-JCNLP 2021, pp. 513–523.

Chen, L., Li, J., Dong, X., Zhang, P., He, C., Wang, J., Zhao, F., Lin, D., 2025. Sharegpt4v: Improving large multi-modal models with better captions, in: European Conference on Computer Vision, Springer. pp. 370–387.

Chen, Z., Wu, J., Wang, W., Su, W., Chen, G., Xing, S., Zhong, M., Zhang, Q., Zhu, X., Lu, L., et al., 2024. Internvl: Scaling up vision foundation models and aligning for generic visual-linguistic tasks, in: Proceedings of the IEEE/CVF conference on computer vision and pattern recognition, pp. 24185–24198.

Chiang, W.L., Li, Z., Lin, Z., Sheng, Y., Wu, Z., Zhang, H., Zheng, L., Zhuang, S., Zhuang, Y., Gonzalez, J.E., et al., 2023. Vicuna: An open-source chatbot impressing gpt-4 with 90%* chatgpt quality. <https://lmsys.org/blog/2023-03-30-vicuna> .

Dai, W., Li, J., Li, D., Tiong, A., Zhao, J., Wang, W., Li, B., Fung, P., Hoi, S., 2023. InstructBLIP: Towards general-purpose vision-language models with instruction tuning, in: Thirty-seventh Conference on Neural Information Processing Systems.

Dong, X., Zhang, P., Zang, Y., Cao, Y., Wang, B., Ouyang, L., Wei, X., Zhang, S., Duan, H., Cao, M., et al., 2024. Internlm-xcomposer2: Mastering free-form text-image composition and comprehension in vision-language large model. arXiv preprint arXiv:2401.16420 .

Gao, J., Pi, R., Zhang, J., Ye, J., Zhong, W., Wang, Y., HONG, L., Han, J., Xu, H., Li, Z., Kong, L., 2025. G-LLaVA: Solving geometric problem with multi-modal large language model, in: The Thirteenth International Conference on Learning Representations.

He, L., Li, Z., Cai, X., Wang, P., 2024. Multi-modal latent space learning for chain-of-thought reasoning in language models, in: Proceedings of the AAAI Conference on Artificial Intelligence, pp. 18180–18187.

Hu, E.J., Shen, Y., Wallis, P., Allen-Zhu, Z., Li, Y., Wang, S., Wang, L., Chen, W., 2022. LoRA: Low-rank adaptation of large language models, in: The Tenth International Conference on Learning Representations.

Hurst, A., Lerer, A., Goucher, A.P., Perelman, A., Ramesh, A., Clark, A., Ostrow, A., Welihinda, A., Hayes, A., Radford, A., et al., 2024. Gpt-4o system card. arXiv preprint arXiv:2410.21276 .

Imani, S., Du, L., Shrivastava, H., 2023. Mathprompter: Mathematical reasoning using large language models. arXiv preprint arXiv:2303.05398 .

Jia, M., Zhang, Z., Yu, W., Jiao, F., Jiang, M., 2024. Describe-then-reason: Improving multimodal mathematical reasoning through visual comprehension training. arXiv preprint arXiv:2404.14604 .

Ke, Z., Jiao, F., Ming, Y., Nguyen, X.P., Xu, A., Long, D.X., Li, M., Qin, C., Wang, P., silvio savarese, Xiong, C., Joty, S., 2025. A survey of frontiers in LLM reasoning: Inference scaling, learning to reason, and agentic systems. Transactions on Machine Learning Research .

Li, B., Zhang, H., Zhang, K., Guo, D., Zhang, Y., Zhang, R., Li, F., Liu, Z., Li, C., 2024. Llava-next: What else influences visual instruction tuning beyond data?

Li, J., Li, D., Savarese, S., Hoi, S., 2023. Blip-2: Bootstrapping language-image pre-training with frozen image encoders and large language models, in: International Conference on Machine Learning, pp. 19730–19742.

Liang, Z., Yang, T., Zhang, J., Zhang, X., 2023. Unimath: A foundational and multimodal mathematical reasoner, in: Proceedings of the 2023 Conference on Empirical Methods in Natural Language Processing, pp. 7126–7133.

Liao, Z., Chen, K., Lin, Y., Li, K., Liu, Y., Chen, H., Huang, X., Yu, Y., 2025. Attack and defense techniques in large language models: A survey and new perspectives. Neural Networks , 108388.

Lin, Z., Liu, C., Zhang, R., Gao, P., Qiu, L., Xiao, H., Qiu, H., Lin, C., Shao, W., Chen, K., et al., 2023. Sphinx: The joint mixing of weights, tasks, and visual embeddings for multi-modal large language models. arXiv preprint arXiv:2311.07575 .

Liu, H., Li, C., Li, Y., Lee, Y.J., 2024a. Improved baselines with visual instruction tuning, in: Proceedings of the IEEE/CVF Conference on Computer Vision and Pattern Recognition, pp. 26296–26306.

Liu, H., Li, C., Wu, Q., Lee, Y.J., 2024b. Visual instruction tuning. Advances in Neural Information Processing Systems 36.

Loshchilov, I., Hutter, F., 2019. Decoupled weight decay regularization, in: The Seventh International Conference on Learning Representations.

Lu, H., Liu, W., Zhang, B., Wang, B., Dong, K., Liu, B., Sun, J., Ren, T., Li, Z., Yang, H., et al., 2024a. Deepseek-vl: towards real-world vision-language understanding. arXiv preprint arXiv:2403.05525 .

Lu, P., Bansal, H., Xia, T., Liu, J., Li, C., Hajishirzi, H., Cheng, H., Chang, K.W., Galley, M., Gao, J., 2024b. Mathvista: Evaluating mathematical reasoning of foundation models in visual contexts, in: The Twelfth International Conference on Learning Representations.

Lu, P., Gong, R., Jiang, S., Qiu, L., Huang, S., Liang, X., Zhu, S.C., 2021. Inter-gps: Interpretable geometry problem solving with formal language and symbolic reasoning, in: Proceedings of the 59th Annual Meeting of the Association for Computational Linguistics, pp. 6774–6786.

Nie, Y., Cui, Q., Li, W., Lü, Y., Yu, W., 2025. A vision-language model for enhanced mci identification in alzheimer’s disease through neuropsychological and neuroimaging data integration. Neural Networks , 108415.

OpenAI, 2023. Gpt-4vision.

Qiao, R., Tan, Q., Dong, G., Wu, M., Sun, C., Song, X., GongQue, Z., Lei, S., Wei, Z., Zhang, M., et al., 2025. We-math: Does your large multimodal model achieve human-like mathematical reasoning?, in: Proceedings of the 63rd Annual Meeting of the Association for Computational Linguistics.

Radford, A., Kim, J.W., Hallacy, C., Ramesh, A., Goh, G., Agarwal, S., Sastry, G., Askell, A., Mishkin, P., Clark, J., et al., 2021. Learning transferable visual models from natural language supervision, in: International Conference on Machine Learning, pp. 8748–8763.

Shi, W., Hu, Z., Bin, Y., Liu, J., Yang, Y., Ng, S.K., Bing, L., Lee, R.K.W., 2024. Math-LLaVA: Bootstrapping mathematical reasoning for multimodal large language models, in: Findings of the Association for Computational Linguistics: EMNLP 2024, pp. 4663–4680.

Sun, T., Chai, L., Yang, J., Yin, Y., Guo, H., Liu, J., Wang, B., Yang, L., Li, Z., 2024. Unicoder: Scaling code large language model via universal code, in: Proceedings of the 62nd Annual Meeting of the Association for Computational Linguistics.

Team, G., Anil, R., Borgeaud, S., Wu, Y., Alayrac, J.B., Yu, J., Soricut, R., Schalkwyk, J., Dai, A.M., Hauth, A., et al., 2023. Gemini: a family of highly capable multimodal models. arXiv preprint arXiv:2312.11805 .

Touvron, H., Lavril, T., Izacard, G., Martinet, X., Lachaux, M.A., Lacroix, T., Rozière, B., Goyal, N., Hambro, E., Azhar, F., et al., 2023a. Llama: Open and efficient foundation language models. arXiv preprint arXiv:2302.13971 .

Touvron, H., Martin, L., Stone, K., Albert, P., Almahairi, A., Babaei, Y., Bashlykov, N., Batra, S., Bhargava, P., Bhosale, S., et al., 2023b. Llama 2: Open foundation and fine-tuned chat models. arXiv preprint arXiv:2307.09288 .

Wang, P., Bai, S., Tan, S., Wang, S., Fan, Z., Bai, J., Chen, K., Liu, X., Wang, J., Ge, W., et al., 2024a. Qwen2-vl: Enhancing vision-language model’s perception of the world at any resolution. arXiv preprint arXiv:2409.12191 .

Wang, Y., Chen, W., Han, X., Lin, X., Zhao, H., Liu, Y., Zhai, B., Yuan, J., You, Q., Yang, H., 2024b. Exploring the reasoning abilities of multimodal large language models (mllms): A comprehensive survey on emerging trends in multimodal reasoning. arXiv preprint arXiv:2401.06805 .

Wang, Z., Han, Z., Chen, S., Xue, F., Ding, Z., Xiao, X., Tresp, V., Torr, P., Gu, J., 2024c. Stop reasoning! when multimodal llms with chain-of-thought reasoning meets adversarial images. arXiv preprint arXiv:2402.14899 .

Xia, R., Li, M., Ye, H., Wu, W., Zhou, H., Yuan, J., Peng, T., Cai, X., Yan, X., Wang, B., et al., 2025. Geox: Geometric problem solving through

unified formalized vision-language pre-training, in: The Thirteenth International Conference on Learning Representations.

Xu, K., Ba, J., Kiros, R., Cho, K., Courville, A., Salakhudinov, R., Zemel, R., Bengio, Y., 2015. Show, attend and tell: Neural image caption generation with visual attention, in: International Conference on Machine Learning, pp. 2048–2057.

Yang, A., Yang, B., Hui, B., Zheng, B., Yu, B., Zhou, C., Li, C., Li, C., Liu, D., Huang, F., Dong, G., Wei, H., Lin, H., Tang, J., Wang, J., Yang, J., Tu, J., Zhang, J., Ma, J., Yang, J., Xu, J., Zhou, J., Bai, J., He, J., Lin, J., Dang, K., Lu, K., Chen, K., Yang, K., Li, M., Xue, M., Ni, N., Zhang, P., Wang, P., Peng, R., Men, R., Gao, R., Lin, R., Wang, S., Bai, S., Tan, S., Zhu, T., Li, T., Liu, T., Ge, W., Deng, X., Zhou, X., Ren, X., Zhang, X., Wei, X., Ren, X., Liu, X., Fan, Y., Yao, Y., Zhang, Y., Wan, Y., Chu, Y., Liu, Y., Cui, Z., Zhang, Z., Guo, Z., Fan, Z., 2024. Qwen2 technical report [arXiv:2407.10671](https://arxiv.org/abs/2407.10671).

Yang, A., Yang, B., Zhang, B., Hui, B., Zheng, B., Yu, B., Li, C., Liu, D., Huang, F., Wei, H., Lin, H., Yang, J., Tu, J., Zhang, J., Yang, J., Yang, J., Zhou, J., Lin, J., Dang, K., Lu, K., Bao, K., Yang, K., Yu, L., Li, M., Xue, M., Zhang, P., Zhu, Q., Men, R., Lin, R., Li, T., Tang, T., Xia, T., Ren, X., Ren, X., Fan, Y., Su, Y., Zhang, Y., Wan, Y., Liu, Y., Cui, Z., Zhang, Z., Qiu, Z., 2025. Qwen2.5 technical report [arXiv:2412.15115](https://arxiv.org/abs/2412.15115).

Ye, Q., Xu, H., Xu, G., Ye, J., Yan, M., Zhou, Y., Wang, J., Hu, A., Shi, P., Shi, Y., et al., 2023. mplug-owl: Modularization empowers large language models with multimodality. arXiv preprint arXiv:2304.14178

Ye, Q., Xu, H., Ye, J., Yan, M., Hu, A., Liu, H., Qian, Q., Zhang, J., Huang, F., 2024a. mplug-owl2: Revolutionizing multi-modal large language model with modality collaboration, in: Proceedings of the IEEE/CVF Conference on Computer Vision and Pattern Recognition, pp. 13040–13051.

Ye, Q., Xu, H., Ye, J., Yan, M., Hu, A., Liu, H., Qian, Q., Zhang, J., Huang, F., 2024b. mplug-owl2: Revolutionizing multi-modal large language model with modality collaboration, in: Proceedings of the IEEE/CVF Conference on Computer Vision and Pattern Recognition, pp. 13040–13051.

Yu, J., He, R., Ying, Z., 2024. Thought propagation: An analogical approach to complex reasoning with large language models, in: The Twelfth International Conference on Learning Representations.

Yuan, L., Cui, G., Wang, H., Ding, N., Wang, X., Deng, J., Shan, B., Chen, H., Xie, R., Lin, Y., et al., 2024. Advancing llm reasoning generalists with preference trees. arXiv preprint arXiv:2404.02078 .

Zeng, J., Zhang, W., Chen, K., Tan, J., Yu, T., Zheng, W.S., Wang, R., 2025. Dual-modality adaptation in vision-language models for continual learning. Neural Networks , 108422.

Zhang, D., Yu, Y., Li, C., Dong, J., Su, D., Chu, C., Yu, D., 2024. MMLMs: Recent advances in MultiModal large language models, in: Findings of the Association for Computational Linguistics: ACL 2024, pp. 12401–12430.

Zhang, E., Yan, X., Lin, W., Zhang, T., Qianchun, L., 2025a. Learning like humans: Advancing llm reasoning capabilities via adaptive difficulty curriculum learning and expert-guided self-reformulation, in: Proceedings of the 2025 Conference on Empirical Methods in Natural Language Processing, pp. 6630–6644.

Zhang, R., Wei, X., Jiang, D., Guo, Z., Zhang, Y., Tong, C., Liu, J., Zhou, A., Zhang, S., Gao, P., Li, H., 2025b. MAVIS: Mathematical visual instruction tuning with an automatic data engine, in: The Thirteenth International Conference on Learning Representations.

Zhang, Y., Zhang, R., Gu, J., Zhou, Y., Lipka, N., Yang, D., Sun, T., 2023. Llavar: Enhanced visual instruction tuning for text-rich image understanding. arXiv preprint arXiv:2306.17107 .

Zheng, G., Yang, B., Tang, J., Zhou, H.Y., Yang, S., 2023. Ddcot: Duty-distinct chain-of-thought prompting for multimodal reasoning in language models. Advances in Neural Information Processing Systems 36, 5168–5191.

Zheng, M., Feng, X., Si, Q., She, Q., Lin, Z., Jiang, W., Wang, W., 2024. Multimodal table understanding, in: Proceedings of the 62nd Annual Meeting of the Association for Computational Linguistics, pp. 9102–9124.

Zhu, D., Chen, J., Shen, X., Li, X., Elhoseiny, M., 2024a. MiniGPT-4: Enhancing vision-language understanding with advanced large language models, in: The Twelfth International Conference on Learning Representations.

Zhu, X., Li, J., Liu, Y., Ma, C., Wang, W., 2024b. Distilling mathematical reasoning capabilities into small language models. Neural Networks 179, 106594.

Zhuang, W., Huang, X., Zhang, X., Zeng, J., 2025. Math-puma: Progressive upward multimodal alignment to enhance mathematical reasoning, in: Proceedings of the AAAI Conference on Artificial Intelligence, pp. 26183–26191.

Zou, H., Wang, Y., Huang, A., 2025. A novel span and syntax enhanced large language model based framework for fine-grained sentiment analysis. Neural Networks , 108012.